J. Biochem. **143,** 555–567 (2008)
doi:10.1093/jb/mvm249

O-Mannosylation is Required for Degradation of the Endoplasmic Reticulum-associated Degradation Substrate Gas1*p *via* the Ubiquitin/Proteasome Pathway in *Saccharomyces cerevisiae*

Hiroto Hirayama[1,2], Morihisa Fujita[1], Takehiko Yoko-o[1] and Yoshifumi Jigami[1,2,*]

[1]Research Institute for Cell Engineering, National Institute of Advanced Industrial Science and Technology (AIST), Tsukuba, Ibaraki 305-8566; and [2]Graduate School of Life and Environmental Science, University of Tsukuba, Tsukuba, Ibaraki 305-8752, Japan

Received November 22, 2007; accepted December 26, 2007; published online January 7, 2008

In *Saccharomyces cerevisiae*, protein *O*-mannosylation, which is executed by protein *O*-mannosyltransferases, is essential for a variety of biological processes as well as for conferring solubility to misfolded proteins. To determine if *O*-mannosylation plays an essential role in endoplasmic reticulum-associated degradation (ERAD) of misfolded proteins, we used a model misfolded protein, Gas1*p. The *O*-mannose content of Gas1*p, which is transferred by protein *O*-mannosyltransferases, was higher than that of Gas1p. Both Pmt1p and Pmt2p, which do not transfer *O*-mannose to correctly folded Gas1p, participated in the *O*-mannosylation of Gas1*p. Furthermore, in a *pmt1*Δ *pmt2*Δ double-mutant background, degradation of Gas1*p is altered from a primarily proteasome dependent to a vacuolar protease-dependent pathway. This process is in a manner dependent on a Golgi-to-endosome sorting function of the *VPS30* complex II. Collectively, our data suggest that *O*-mannosylation plays an important role for proteasome-dependent degradation of Gas1*p via the ERAD pathway and when *O*-mannosylation is insufficient, Gas1*p is degraded in the vacuole. Thus, we propose that *O*-mannosylation by Pmt1p and Pmt2p might be a key step in the targeting of some misfolded proteins for degradation via the proteasome-dependent ERAD pathway.

Key words: ERAD, Gas1*p, *O*-mannosylation, *PMT*, post-ER degradation.

Abbreviations: CHX, cycloheximide; CPY*, mutant carboxypeptidase Y; ER, endoplasmic reticulum; ERAD, endoplasmic reticulum-associated degradation; GPI, glycosylphosphatidylinositol; HA, haemagglutinin; mutant pαF, mutant pro-α-factor; KHN, Kar2p signal sequence fused to simian virus 5 haemagglutinin neuraminidase; KHNt, HA-tagged yeast Kar2p signal sequence fusion to simian virus 5 haemagglutinin neuraminidase; PNGase F, peptide *N*-glycanase F; Δpro, pro-region-deleted derivative of *Rhizopus niveus* aspartic proteinase-I; sol-Gas1*p, non-GPI-anchored soluble version of Gas1*p.

Endoplasmic reticulum (ER) quality-control systems participate in correct protein folding. Moreover, ER quality-control systems decrease cell toxicity and prevent cell death due to the accumulation of aberrantly folded proteins in the ER by removing misfolded proteins (*1*). ER molecular chaperones [*e.g.* heavy chain-binding protein (BiP), calnexin and protein disulphide isomerase (PDI)] facilitate the folding of newly synthesized proteins.

The addition of *N*-linked oligosaccharides is a major protein modification and contributes to correct folding of glycoproteins. $Glc_3Man_9GlcNAc_2$, which is transferred to Asn-X-Ser/Thr sequences of nascent polypeptide chains, is trimmed and processed by glucosidase I, glucosidase II and mannosidase I, converting it to $Man_8GlcNAc_2$ (*2*, *3*). In mammalian systems, the intermediate of the trimming process, $Glc_1Man_9GlcNAc_2$, is capable of interacting with the lectin-like molecular chaperone calnexin/calreticulin. This interaction promotes the correct folding of newly synthesized glycoproteins in the ER (*4*). Yeast *Saccharomyces cerevisiae* has an orthologue of calnexin, Cne1p. However, Cne1p activity is not essential for the folding of glycoprotein in yeast cells (*5*), even though Cne1p is capable of interacting with $Glc_1Man_9GlcNAc_2$ structure *in vitro* (*6*). Incorrectly folded proteins in the ER are degraded by the 26S proteasome after retrotranslocation into the cytosol and ubiquitination. This process is called ER-associated degradation (ERAD) (*7*, *8*). In addition, some misfold secreted proteins appear to be targeted to the vacuole and degraded in a vacuolar protease-dependent manner (post-ER degradation) (*9*–*14*). In post-ER degradation, misfolded model proteins, which are degraded by vacuolar proteases, are targeted to the vacuole *via* two routes, namely, the Golgi-to-vacuole sorting pathway (*15*) and the autophagic pathway (*16*).

In addition to modification with *N*-linked sugar chains, some proteins are modified with *O*-mannoses. The first mannose of *O*-linked sugar chains is transferred by protein *O*-mannosyltransferases (Pmts) in the ER. The transfer of *O*-mannose to serine/threonine residues of proteins by Pmts is evolutionally conserved in various eukaryotic organisms from fungi to human and found even in bacterial species

*To whom correspondence should be addressed. Tel: +81 29 861 6160, Fax: +81 29 861 6161, E-mail: jigami.yoshi@aist.go.jp

(*e.g*. *Mycobacterium tuberculosis*) (*17–22*). In the budding yeast, *S. cerevisiae*, Pmt1p–Pmt6p are involved in the transfer of a mannose to serine or threonine residues using dolichol phosphate mannose as a mannosyl donor (*23*). Pmt1p–Pmt6p have been classified into three subfamilies, *PMT1*, *PMT2* and *PMT4* (*17*). Additionally, members of the *PMT1* subfamily (Pmt1p and Pmt5p) reportedly interact in pairs with members of the *PMT2* subfamily (Pmt2p and Pmt3p) to form heterodimeric complexes (Pmt1p–Pmt2p, Pmt3p–pmt5p) and the *PMT4* subfamily proteins reportedly form homomeric complexes (Pmt4p–Pmt4p) (*24*). These complexes, which are essential for mannosyltransferase activity, have different substrate specificity and catalyse the *O*-mannose transfer reaction differently in response to different acceptor protein substrates *in vivo* (*25*). *O*-mannosylation is known to play an important role in various biological processes, including protein stability (*26*, *27*), protein secretion (*20*, *28*), cell-wall integrity (*29*) and the budding process (*30*). It has also been reported that a small portion of pro-α-factor mutant (mutant pαF) and a pro-region-deleted derivative of *Rhizopus niveus* aspartic proteinase-I (Δpro) are *O*-mannosylated by Pmt1p and/or Pmt2p (*31*, *32*). More specifically, Δpro takes *O*-mannosylation only when some components of ERAD machinery are abolished (*32*), and another ERAD substrate, the Kar2p signal sequence fused to simian virus 5 haemagglutinin neuraminidase (KHN), is also *O*-mannosylated by Pmt1p and/or Pmt2p when expressed in yeast cells (*33*). The *O*-mannosylation of misfolded proteins such as mutant pαF and Δpro enhances their solubility, preventing them from aggregation in the ER (*32*). However, degradation of mutant pαF and Δpro is not affected by mutation of *PMT1* or *PMT2* (*31*, *32*). Therefore, it remains unclear if *O*-mannosylation of misfolded proteins plays an essential role in ERAD pathways.

The glycosylphosphatidylinositol (GPI)-anchored protein Gas1p functions as a glucanosyltransferase on the plasma membrane and is modified by both *N*- and *O*-glycosylation (*34*). We previously generated Gas1*p, a misfolded ERAD substrate, and demonstrated that deacylation of the GPI anchor is important for the degradation of Gas1*p (*35*). In the current study, we dissected the molecular role of *O*-mannosylation in degradation of misfolded proteins using Gas1*p and a non-GPI-anchored soluble version of Gas1*p (sol-Gas1*p). We found that Gas1*p is excessively *O*-mannosylated as compared to Gas1p. Pmt1p and Pmt2p, which are not responsible for *O*-mannosylation of correctly folded Gas1p, participate in *O*-mannosylation of Gas1*p. We further found that in cells lacking both Pmt1p and Pmt2p function (*pmt1*Δ *pmt2*Δ), Gas1*p is transported to the vacuole *via* the endosomal sorting process, and degradation of Gas1*p shifts from a proteasome-dependent (ubiquitin/proteasome ERAD) to a vacuolar protease-dependent (post-ER degradation) pathway. These results support the idea that *O*-mannosylation of Gas1*p as catalysed by Pmt1p and Pmt2p plays a crucial role in degradation of Gas1*p through the ERAD pathway, which is dependent on proteasome degradation, and that vacuolar protease-dependent degradation of Gas1*p is facilitated in a *pmt1*Δ *pmt2*Δ double-mutant background.

MATERIALS AND METHODS

Strains, Growth Conditions and Gene Disruption—The yeast strains used in this study are listed in Table 1. Gene disruption in yeast cells was performed by the one-step PCR method (*36*). Cells were grown in YPAD medium, synthetic dextrose medium (*37*) and SCD medium (0.67% yeast nitrogen base without amino acids, 0.5% casamino acids and 2% glucose) with appropriate nutritional supplements. Metabolic labelling experiments using [^{35}S]-cysteine/methionine were carried out in synthetic medium with a low SO_4^{2-} concentration (0.17% yeast nitrogen base without amino acids and ammonium sulphate, 0.5% casamino acids, 5% glucose, nutritional supplements and 200 μM ammonium sulphate) and synthetic medium lacking methionine, cysteine and ammonium sulphate (0.17% yeast nitrogen base without amino acids and ammonium sulphate, 0.5% casamino acids, 5% glucose and nutritional supplements without cysteine and methionine). For osmotic stabilization, each medium was supplemented with 300 mM KCl.

Plasmids used in this Study—The plasmids used were as follows. The pSM70 plasmid, which contains the yeast Kar2p signal sequence fused to simian virus 5 haemagglutinin neuraminidase, with an HA-tag inserted at the COOH-terminal; the KHNt expression vector, which was a gift from Davis Ng (National University of Singapore, Singapore) (*33*); and pMF848 (HA-tagged *prc1-1*, *URA3*), which is described elsewhere (*35*). The HA-Gas1p expression plasmid, pHI101 and the HA-Gas1*p expression plasmid, pHI102, were constructed as follows. Plasmids pMF600 (*HA*-tagged *GAS1*, *URA3*) (*35*) and pMF605 (*HA*-tagged *gas1-871,873*, *URA3*) (*35*) were digested with *Bam*HI and *Sac*II. The fragments containing haemagglutinin (*HA*)-tagged *GAS1* and *HA*-tagged *gas1-871,873* were ligated into pRS316 (*CEN*/*ARS*, *URA3*) (*38*) to generate pHI101 (HA-tagged *GAS1*, *CEN*/*ARS*, *URA3*), and pHI102 (*HA*-tagged *gas1-871,873*, *CEN*/*ARS*, *URA3*), respectively. To construct plasmids expressing non-GPI-anchored HA-Gas1p (HA-sol-Gas1p) and HA-Gas1*p (HA-sol-Gas1*p), the plasmids pMF876 (*HA*-tagged sol-*GAS1*, *URA3*) (*35*) and pMF874 (*HA*-tagged sol-*gas1-871,873*, *LEU2*) (*35*) were digested with *Bam*HI and *Spe*I, and fragments encoding HA-tagged sol-Gas1p and HA-tagged sol-Gas1*p were ligated into pRS316 (*CEN*/*ARS*, *URA3*) to generate pHI118 (*HA*-tagged sol-*GAS1*, *CEN*/*ARS*, *URA3*) and pHI119 (*HA*-tagged sol-*gas1-871,873*, *CEN*/*ARS*, *URA3*), respectively.

Pulse-chase and Immunoprecipitation Experiments—Cells were grown to a logarithmic phase of growth in synthetic medium with low SO_4^{2-}. Then, 15 OD_{600} units of cells were washed and resuspended in 3 ml of the synthetic medium lacking methionine, cysteine and ammonium sulphate. After 20–40 min of incubation at 30°C, cells were pulse-labelled with 30 μCi Pro-mix-L [^{35}S] *in vitro* cell labelling mix (GE Healthcare Life

Table 1. **Yeast strains used in this study.**

Strain	Harbouring plasmid	Genotype	Source
W303-1A	–	*MAT***a** *leu2-3,112 his3-11 ade2-1 ura3-1 trp1-1 can1-100*	(*56*)
YJY1	–	*MAT***a** *his3Δ1 leu2Δ0 met15Δ0 ura3Δ0* (S288C background)	Lab strain
BY4741	–	*MAT***a** *his3Δ1 leu2Δ0 met15Δ0 ura3Δ0*	ATCC
BY4742	–	*MATα his3Δ1 leu2Δ0 lys2Δ0 ura3Δ0*	ATCC
SSY18	–	*MAT***a** *ktr1Δ::hisG kre2Δ::hisG ktr3Δ::hisG* W303	Lab strain
YME1305	pHI102	*MAT***a** YJY1	This study
pmt1Δ	–	*MAT***a** *pmt1Δ::kanMX6* BY4741	SDP
pmt2Δ	–	*MAT***a** *pmt2Δ::kanMX6* BY4741	SDP
pmt3Δ	–	*MAT***a** *pmt3Δ::kanMX6* BY4741	SDP
pmt4Δ	–	*MAT***a** *pmt4Δ::His3MX6* YJY1	This study
pmt5Δ	–	*MAT***a** *pmt5Δ::kanMX6* BY4741	SDP
pmt6Δ	–	*MAT***a** *pmt6Δ::kanMX6* BY4741	SDP
YME318	pHI101	*MAT***a** SSY18	This study
YME319	pHI102	*MAT***a** SSY18	This study
YME335	pHI118	*MAT***a** SSY18	This study
YME336	pHI119	*MAT***a** SSY18	This study
YME1315	pHI102	*MAT***a** *pmt1Δ::kanMX6* BY4741	This study
YME1316	pHI102	*MAT***a** *pmt2Δ::kanMX6* BY4741	This study
YME1317	pHI102	*MAT***a** *pmt3Δ::kanMX6* BY4741	This study
YME1334	pHI102	*MAT***a** *pmt4Δ::His3MX6* YJY1	This study
YME1318	pHI102	*MAT***a** *pmt5Δ::kanMX6* BY4741	This study
YME1319	pHI102	*MAT***a** *pmt6Δ::kanMX6* BY4741	This study
YME1336	pHI102	*MAT***a** *pmt1Δ::His3MX6 pmt2Δ::kanMX6* BY4741	This study
YME1374	pHI102	*MAT***a** *pmt4Δ::His3MX6 pmt6Δ::kanMX6* BY4741	This study
YME1384	pHI102	*MAT***a** *pep4Δ::His3MX6* BY4741	This study
YME1385	pHI102	*MAT***a** *pep4Δ::LEU2 pmt1Δ::His3MX6 pmt2Δ::kanMX6* BY4741	This study
YME1392	pHI102	*MAT***a** *pep4Δ::LEU2 pmt4Δ::His3MX6 pmt6Δ::kanMX6* BY4741	This study
YME1398	pHI119	*MAT***a** BY4741	This study
YME1399	pHI119	*MATα pep4Δ::LEU2* BY4742	This study
YME1400	pHI119	*MAT***a** *pep4Δ::LEU2 pmt1Δ::His3MX6 pmt2Δ::kanMX6* BY4741	This study
YME1421	pMF848	*MAT***a** BY4741	This study
YME1422	pMF848	*MATα pep4Δ::LEU2* BY4742	This study
YME1423	pMF848	*MAT***a** *pep4Δ::LEU2 pmt1Δ::His3MX6 pmt2Δ::kanMX6* BY4741	This study
YME1425	pHI119	*MAT***a** BY4741	This study
YME1426	pHI119	*MAT***a** *pmt1Δ::kanMX6* BY4741	This study
YME1427	pHI119	*MAT***a** *pmt2Δ::kanMX6* BY4741	This study
YME1428	pHI119	*MAT***a** *pmt3Δ::kanMX6* BY4741	This study
YME1429	pHI119	*MAT***a** *pmt4Δ::His3MX6* YJY1	This study
YME1430	pHI119	*MAT***a** *pmt5Δ::kanMX6* BY4741	This study
YME1431	pHI119	*MAT***a** *pmt6Δ::kanMX6* BY4741	This study
YME1440	pHI102	*MATα vps38Δ::His3MX6 pmt1Δ::LEU2 pmt2Δ::kanMX6 ura3Δ0 lys2Δ0*	This study
YME1444	pHI102	*MAT***a** *vps38Δ::kanMX6* BY4741	This study
YME1445	pSM70	*MAT***a** BY4741	This study
YME1446	pSM70	*MAT***a** *pmt1Δ::His3MX6 pmt2Δ::kanMX6* BY4741	This study
YME1447	pSM70	*MAT***a** *pep4Δ::LEU2 pmt1Δ::His3MX6 pmt2Δ::kanMX6* BY4741	This study

SDP, *Saccharomyces* Deletion Project (http://www-deletion.stanford.edu/YDPM/index.html); ATCC, American Type Culture Collection; Lab strain, laboratory strain.
The following plasmids were generated in this study: pHI101 (*HA*-tagged *GAS1*, *CEN*/*ARS*, *URA3*), pHI102 (*HA*-tagged *gas1-871,873*, *CEN*/*ARS*, *URA3*), pHI118 (*HA*-tagged sol-*GAS1*, *CEN*/*ARS*, *URA3*), pHI119 (*HA*-tagged sol-*gas1-871,873*, *CEN*/*ARS*, *URA3*), pMF848 (*HA*-tagged *prc1-1*, *CEN*/*ARS*, *URA3*) and pSM70 (*HA*-tagged-KHN driven by *PRC1* promoter, *CEN*/*ARS*, *URA3*).

Sciences, Piscataway, NJ, USA) for 10 min. The chase phase was initiated by the addition of 1/100 vol of chase cocktail (0.3% methionine, 0.3% cysteine and 0.3 M ammonium sulphate). The chase was terminated by addition of NaF and NaN_3 to a final concentration of 10 mM each. Preparation of cell lysate, immunoprecipitation and SDS–PAGE were performed as described previously (*39*). For peptide *N*-glycanase F (PNGase F) digestion, samples were resuspended in denaturing buffer [0.5% SDS and 40 mM dithiothreitol (DTT)] and boiled for 10 min. Next, reaction buffer [0.5 M sodium phosphate (pH 7.5), 1% NP-40 and protease inhibitor cocktail (Roche, Basel, Switzerland)] was added, and the reaction mixture was treated with 125 U of PNGase F (New England Biolabs, Herts, UK) for 3 h at 37°C. Molecular Imager FX software (Bio-Rad, Hercules, CA, USA) was used for quantification of SDS–PAGE gel bands.

Cycloheximide (CHX) Chase Analysis—CHX-chase analysis for yeast cells was performed as described previously (*35*).

Protein Extraction and Immunoblot Analysis—Yeast cells were grown to a logarithmic phase. Next, 1.0–5.0 OD_{600} units of cells were washed twice, resuspended in 100 μl of TEGN buffer [50 mM Tris–HCl (pH 7.5), 100 mM NaCl, 1 mM EDTA, 1% (w/v) NP-40 and protease inhibitor cocktail (Roche)], and disrupted with glass beads. After removing cell debris by centrifugation, cell lysates were denatured with sample buffer [125 mM Tris–HCl (pH6.8), 4% SDS, 20% glycerol and 3.1% DTT] for 5 min at 98°C. A protein spin concentrator (Orbital Biosciences, Topsfield, MA, USA) was used to concentrate a culture broth of *ktr1*Δ *kre2*Δ *ktr3*Δ cells expressing HA-sol-Gas1p (YME335). The concentrated culture broth was denatured as described earlier. Samples were separated by SDS–PAGE using 7.5% acrylamide gels. Proteins were transferred to PVDF membranes and blocked in TTBS [25 mM Tris–HCl (pH 7.4), 150 mM NaCl and 0.1% (v/v) Tween-20] containing 0.5% (w/v) skimmed milk. Gas1p was detected with anti-Gas1p polyclonal rabbit antiserum (1 : 2,000; kindly provided by K. Hata, Eisai Co., Ltd., Tokyo, Japan) followed by horseradish peroxidase (HRP)-conjugated anti-rabbit IgG antibody (1 : 2,000; Invitrogen, Carlsbad, CA, USA). HA-tagged protein was detected with anti-HA mouse monoclonal antibody 16B12 (1:10,000; Covance, Princeton, NJ), followed by HRP-conjugated goat anti-mouse IgG antibody (1:10,000). Immunoreactive bands were detected by chemiluminescence with ECL Plus reagents (GE Healthcare Life Sciences).

Sucrose Density Gradient Analysis—Cell extracts expressing HA-sol-Gas1*p were prepared as described earlier (see Protein Extraction and Immunoblot Analysis section). The extracts were resuspended in 400 μl of TEG buffer [50 mM Tris–HCl (pH 7.5), 100 mM NaCl, 1 mM EDTA and protease inhibitor cocktail (Roche)] and then solubilized for 30 min at 4°C by addition of Triton X-100 to a final concentration of 1% (w/v). The suspension was centrifuged at 20,000*g* for 30 min to remove insoluble membranes. The supernatant (300 μg of protein) was loaded onto a 5–50% (w/v) sucrose gradient and centrifuged at 145,000*g* for 20 h at 4°C, after which 150–200 μl fractions were collected from the bottom of the gradient and denatured with the sample buffer. An aliquot (10 μl) of each fraction was separated by SDS–PAGE and analysed by immunoblotting using anti-HA antibody (1:8,000), followed by HRP-conjugated anti-mouse IgG antibody (1:8,000). Molecular masses were estimated by comparison of the migration of proteins with the following standards: ferritin (440 kDa), catalase (232 kDa), aldolase (158 kDa) and ovalbumin (43 kDa).

Analysis of Protein Aggregates—Protein aggregate analysis was done using non-ionic detergent as described by Spear and Ng (*40*), with some modifications. Wild-type cells expressing KHNt (YME1445), *pmt1*Δ *pmt2*Δ cells expressing KHNt (YME1446) and *pep4*Δ *pmt1*Δ *pmt2*Δ cells expressing KHNt (YME1447) were grown to a logarithmic phase in SCD medium. Then, 5.0 OD_{600} units of cells were collected by centrifugation and cell extracts were prepared as described above (see Protein Extraction and Immunoblot Analysis section). Cell extracts resuspended in TEG buffer were solubilized for 60 min at 4°C by the addition of Triton X-100 to a final concentration of 1% (w/v). Half of the solubilized total cell extract was kept at 4°C. The remaining half was centrifuged at 20,000*g* for 30 min, the supernatant was removed and the pellet was resuspended in TEG buffer. Finally, the total cell extract, supernatant and pellet fractions were denatured with the sample buffer and 10 μl of each sample was resolved by SDS–PAGE.

RESULTS

Excessive O*-Mannosylation of Gas1*p in the ER*—Gas1p is an *N*-glycosylated protein that contains 10 potential *N*-glycosylation sites (Asn-X-Ser/Thr) and is a highly *O*-mannosylated GPI-anchored protein (*41*, *42*). The misfolded form of Gas1p referred to as Gas1*p has a single amino acid substitution (G291R) and is degraded by the proteasome as an ERAD substrate (*35*). Furthermore, efficient degradation of Gas1*p is dependent on ER-to-Golgi trafficking (*35*) as has been reported for some other misfolded proteins, including mutant carboxypeptidase Y (CPY*) and KHN (*33*, *43*).

We first asked if there is a difference in the extent of *O*-mannosylation of HA-Gas1p and HA-Gas1*p by Pmts. To do this, we carried out experiments in cells with deletions of *KTR1, KRE2* and *KTR3* (*ktr1*Δ *kre2*Δ *ktr3*Δ triple-mutant cells), genes that encode α-1,2-mannosyltranserases involved in addition of the second and third mannose residues of *O*-linked sugar chains (Fig. 1A) and addition of outer chain mannose residues of *N*-glycan in the Golgi apparatus (*44*). Because Gas1p and Gas1*p take *O*-mannose modification through their transport to the Golgi, the molecular weights of HA-Gas1p and HA-Gas1*p include the influence of *N*- and *O*-glycan modification in Golgi apparatus. We compared the molecular weights of Gas1p and Gas1*p after digestion of *N*-glycan by PNGase F in *ktr1*Δ *kre2*Δ *ktr3*Δ triple-mutant cells. After digestion of *N*-glycan, the content of *O*-mannosylated serine/threonine residues is reflected on the difference in molecular weight between Gas1p and Gas1*p. We previously reported that the amount of intracellular Gas1*p is less than that of Gas1p in steady-state cells, because of an ERAD-dependent rapid degradation of Gas1*p (*35*). To detect a small difference in electrophoretic mobility between Gas1p and Gas1*p, we applied four times concentrated cell lysate samples of HA-Gas1*p than those of HA-Gas1p. Prior to digestion with PNGase F, the molecular weight of HA-Gas1p was higher than that of HA-Gas1*p (Fig. 1B, lanes 1 and 2). This difference in molecular weight was presumably due to difference in the extent of elongation of *N*-linked sugar chains. In other words, the *N*-linked sugar chains on the mature HA-Gas1p were modified completely *via* the post-ER secretory pathway, whereas the *N*-linked sugar chains of HA-Gas1*p were only partially modified in the Golgi apparatus. However, HA-Gas1*p had a higher molecular weight than HA-Gas1p after *N*-glycan digestion with PNGase F (Fig. 1B, lanes 3 and 4). Because the

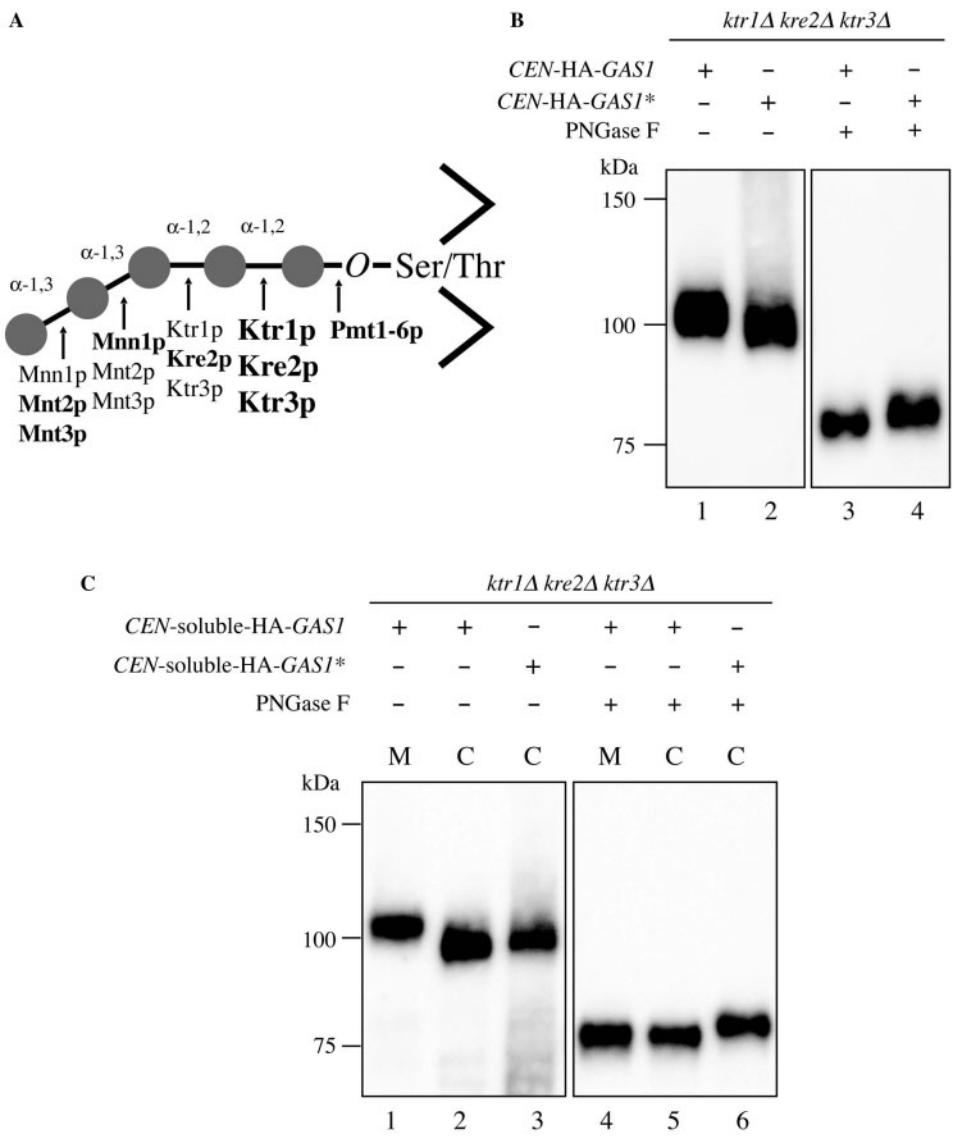

Fig. 1. **The misfolded proteins HA-Gas1*p and HA-sol-Gas1*p contain more *O*-mannosylated residues than correctly folded Gas1p.** (A) The structure of *O*-linked sugar chain in *S. cerevisiae*. Pmt family adds the first mannose on Ser/Thr residues in the ER. α-1,2-mannosyltrasferases Ktr1p, Kre2p and Ktr3p transfer to the second mannose to the mannose residues which is transferred by Pmt family. The principal enzymes in each step are represented in bold face. Closed-circles indicate mannose residues. (B) One OD_{600} unit of *ktr1*Δ *kre2*Δ *ktr3*Δ cells expressed in HA-Gas1p (YME318) and 4.0 OD_{600} units of that in HA-Gas1*p (YME319) were collected and washed with ice-cold water. Whole-cell extracts were prepared as described in MATERIALS AND METHODS section. The same volumes (5 μl) of cell extract were treated with (+) or without (−) PNGase F and denatured with the sample buffer. These samples were separated by SDS–PAGE and visualized by immunoblotting using anti-HA antibody. (C) Immunoblot analyses of *ktr1*Δ *kre2*Δ *ktr3*Δ cells expressing HA-sol-Gas1p (YME335) and HA-sol-Gas1*p (YME336). We prepared 1.0 OD_{600} unit of YME335 cells, 4.0 OD_{600} units of YME336 cells and 1 ml of 5-fold enriched culture medium, in which YME335 cells were grown, and 5 μl of each sample was analysed as described in Fig. 1B. M and C refer to culture medium and cell extract, respectively.

cells lack *KTR1*, *KRE2* and *KTR3*, the difference in molecular weight between HA-Gas1p and HA-Gas1*p after the PNGase F digestion should reflect differences in *O*-linked first mannose content. These results suggest that HA-Gas1*p contains more *O*-mannosylated serine/threonine residues than HA-Gas1p.

Previous findings indicated that HA-Gas1*p is indeed modified by GPI (*35*). Thus, we next examined whether excessive *O*-mannosylation of HA-Gas1*p depends on GPI modification using the same assay in conjunction with expression of non-GPI-attached Gas1p (HA-sol-Gas1p) and Gas1*p (HA-sol-Gas1*p), which were constructed by insertion of a stop codon just before the GPI attachment signal sequence. Since the amount of intracellular HA-sol-Gas1*p is smaller than that of HA-sol-Gas1p per cell, we used 4-fold concentrated samples for HA-sol-Gas1*p using *ktr1*Δ *ker2*Δ *ktr3*Δ triple-mutant cells. After PNGase F treatment, HA-sol-Gas1*p

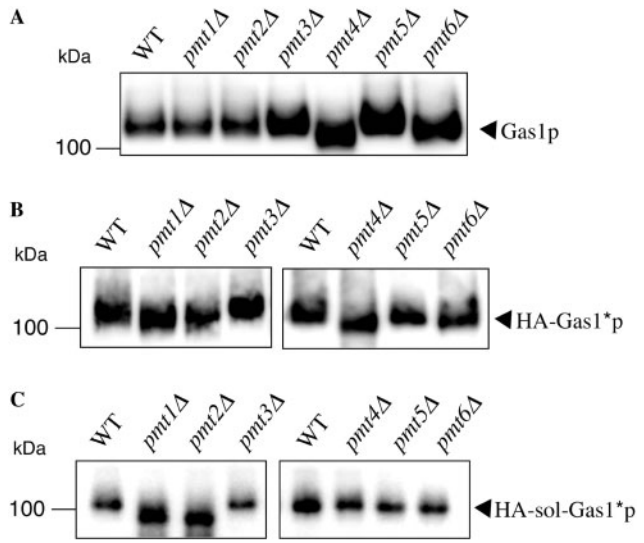

Fig. 2. **In addition to Pmt4p and Pmt6p, Pmt1p and Pmt2p are responsible for *O*-mannosylation of HA-Gas1*p but not of correctly folded Gas1p.** Whole-cell extracts were prepared from 5.0 OD_{600} units of log-phase cultivated cells. (A) Gas1p extracts (10 μl) from wild-type cells (WT; YJY1) and *pmt1*Δ–*pmt6*Δ mutant cells were denatured with sample buffer and subjected to SDS–PAGE, followed by immunoblotting with anti-Gas1p antiserum. (B) Immunoblot analysis of HA-Gas1*p expressed in wild-type (YME1305), *pmt1*Δ (YME1315), *pmt2*Δ (YME1316), *pmt3*Δ (YME1317), *pmt4*Δ (YME1334), *pmt5*Δ (YME1318) and *pmt6*Δ (YME1319) mutant cells. These samples were prepared as described in (A) and detected with an anti-HA antibody. (C) The samples of wild-type (YME1425) and *pmt1*Δ–*pmt6*Δ (YME1426–YME1431) cells expressing HA-sol-Gas1*p were prepared as described in (A) and analysed with an anti-HA antibody.

had a higher molecular weight than those of secreted HA-sol-Gas1p and intracellular HA-sol-Gas1p (Fig. 1C, lanes 4–6), indicating that not only GPI-anchored Gas1*p but also non-GPI-anchored Gas1*p (sol-Gas1*p) contains more *O*-mannosylated serine/threonine residues than correctly folded Gas1p or sol-Gas1p.

*Pmt1p and Pmt2p are Responsible for O-Mannosylation of Gas1*p*—Because there are more *O*-mannosylated sites in both HA-Gas1*p and HA-sol-Gas1*p than in HA-Gas1p and HA-sol-Gas1p, we next sought to determine if Gas1p and Gas1*p are *O*-mannosylated by different Pmt proteins using cells with deletions of single *pmt* genes. Gas1p was under-glycosylated in *pmt4*Δ and *pmt6*Δ cells (Fig. 2A) as reported previously (*25*), whereas HA-Gas1*p was under-glycosylated in *pmt1*Δ and *pmt2*Δ mutant cells (Fig. 2B) as well as in *pmt4*Δ and *pmt6*Δ mutant cells. Moreover, HA-Gas1*p expressed in both *pmt1*Δ *pmt2*Δ and *pmt4*Δ *pmt6*Δ double-deletion mutant cells was more under-glycosylated than that expressed in either single deletion mutant strain (data not shown).

We next used this method to further investigate which Pmt proteins are responsible for the *O*-mannosylation of HA-sol-Gas1*p. Interestingly, we observed under-glycosylation of HA-sol-Gas1*p in *pmt1*Δ and *pmt2*Δ cells, whereas glycosylation of HA-sol-Gas1*p was not affected by the deletion of *PMT4* and *PMT6* genes (Fig. 2C). The result that Pmt4p is not involved in the mannosylation of HA-sol-Gas1*p is consistent with a recent report that Pmt4p specifically mannosylates several transmembrane proteins and GPI-anchored proteins, including Fus1p and Gas1p, whereas non-transmembrane forms of Fus1p ($FUSw/oTM^{ZZ}$) and non-GPI-attached Gas1p ($GAS1\Delta GPI^{ZZ}$) are not *O*-mannosylated by Pmt4p (*45*). These observations also support that Pmt1p and Pmt2p participate in *O*-mannosylation of the misfolded proteins Gas1*p and sol-Gas1*p.

*Gas1*p Expressed in* pmt1Δ pmt2Δ *Double-Mutant Cells is Degraded by Vacuolar Protease*—Because Gas1*p was *O*-mannosylated by Pmt1p and Pmt2p as well as by Pmt4p and Pmt6p, we suspected that the *O*-mannosylation of Gas1*p that is mediated by Pmt1p and Pmt2p plays a different physiological role than that mediated by Pmt4p and Pmt6p. To address this possibility, we compared the rate of degradation of HA-Gas1*p in wild-type, *pmt1*Δ *pmt2*Δ and *pmt4*Δ *pmt6*Δ cells. As shown in Fig. 3A and C, the rate of degradation of HA-Gas1*p was similar in wild-type, *pmt1*Δ *pmt2*Δ and *pmt4*Δ *pmt6*Δ cells.

Gas1*p is degraded by the proteasome (*35*). However, it is known that some misfolded soluble proteins exit the ER and are degraded in the vacuole instead (*9–11*). To determine if HA-Gas1*p in *pmt* mutants is degraded by vacuolar proteases, we examined the kinetics of degradation of HA-Gas1*p in cells lacking a vacuolar protease (*pep4*Δ) and in cells lacking both vacuolar protease and protein *O*-mannosyltransferases (*pep4*Δ *pmt1*Δ *pmt2*Δ and *pep4*Δ *pmt4*Δ *pmt6*Δ). Notably, degradation of HA-Gas1*p was significantly delayed in *pep4*Δ *pmt1*Δ *pmt2*Δ cells (Fig. 3B), whereas degradation of HA-Gas1*p in *pep4*Δ cells was not affected as compared to wild-type cells, as shown in our previous report (*35*). Furthermore, degradation of HA-Gas1*p expressed in *pep4*Δ *pmt4*Δ *pmt6*Δ cells was not delayed (Fig. 3B and D).

To further address a possible delay in degradation of HA-sol-Gas1*p, we performed a CHX-chase experiment for HA-sol-Gas1*p expressed in wild-type, *pep4*Δ and *pep4*Δ *pmt1*Δ *pmt2*Δ cells. As shown in Fig. 4A, HA-sol-Gas1*p was stable in triple gene-disrupted cells (*pep4*Δ *pmt1*Δ *pmt2*Δ), in contrast to what was observed for wild-type and *pep4*Δ cells. These results strongly suggest that the defect in *O*-mannosylation of Gas1*p, which is mediated by Pmt1p and Pmt2p, leads to vacuolar protease-dependent degradation of Gas1*p, which is independent of GPI-anchor modification.

Degradation of CPY is not Affected by Defects in Pmt1p or Pmt2p*—It has been reported that a defect in the ERAD machinery facilitates the anterograde transport of CPY* such that CPY* is finally degraded by the vacuole-localized protease (*46*) and that a defect in Pmt2p leads to activation of the unfolded protein response (*32*). Given these reports, we suspect that vacuolar protease-dependent degradation of HA-Gas1*p is an indirect effect resulting from general ER stress caused by deletion of *PMT1* and *PMT2*. To investigate this possibility, we examined degradation of CPY*, which has been extensively studied as an ERAD substrate in yeast (*47*, *48*) and is modified at four sites by *N*-glycan

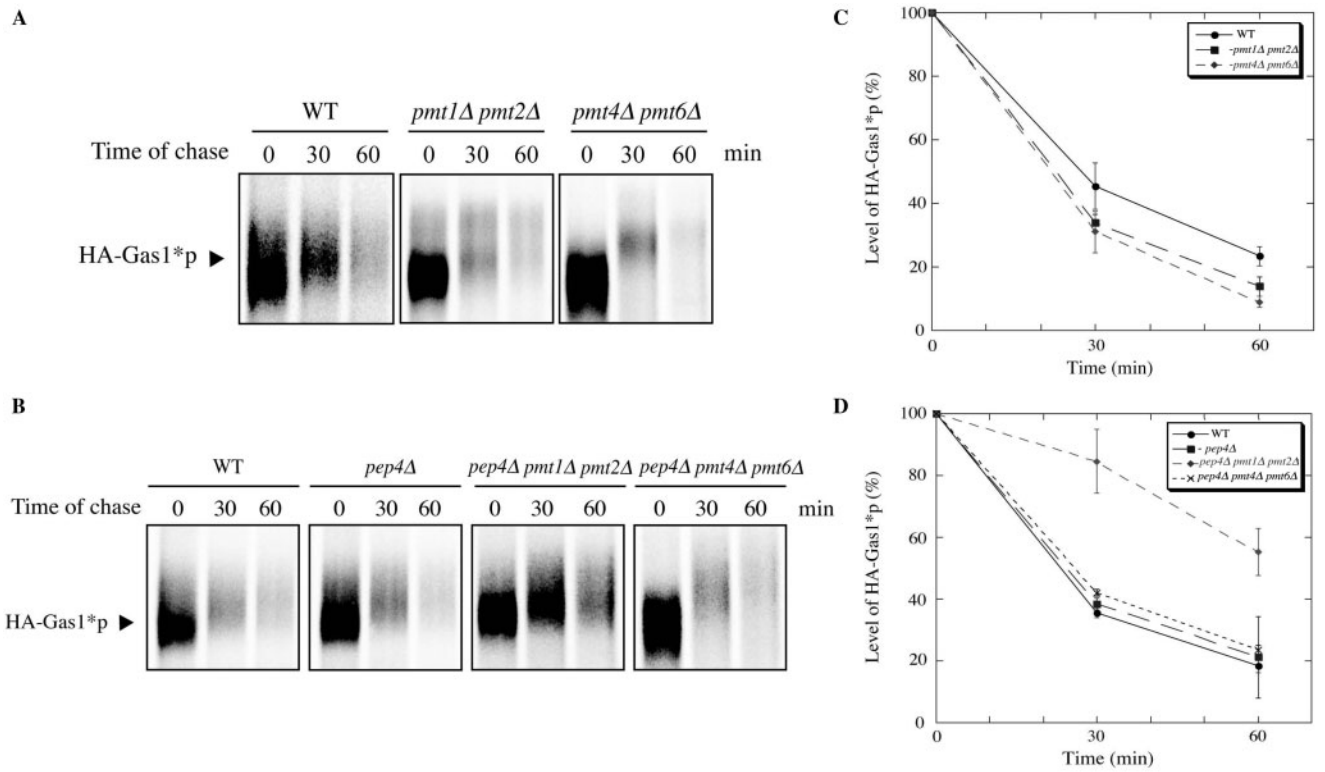

Fig. 3. **HA-Gas1*p expressed in *pmt1*Δ *pmt2*Δ cells is degraded in the vacuole.** (A, B) HA-Gas1*p expressed in wild-type (YME1305), *pmt1*Δ *pmt2*Δ (YME1336), *pmt4*Δ *pmt6*Δ (YME1374), *pep4*Δ (YME1384), *pep4*Δ *pmt1*Δ *pmt2*Δ (YME1385) and *pep4*Δ *pmt4*Δ *pmt6*Δ (YME1392) cells were pulse-labelled with [^{35}S]-cysteine/methionine for 10 min and chased for the indicated amounts of time. HA-Gas1*p was recovered from cell lysates by immunoprecipitation using anti-HA agarose beads and treated with PNGase F for 3 h at 37°C. The samples were separated by SDS–PAGE and detected by autoradiography. (C, D) The percentages of HA-Gas1*p bands relative to the band of time point 0. Error bars indicate mean values ± SD from three independent experiments.

but is not *O*-mannosylated. The kinetics of degradation of CPY*-HA were assessed in wild-type, *pep4*Δ and *pep4*Δ *pmt1*Δ *pmt2*Δ cells by CHX-chase analysis. We found that the degradation kinetics of CPY*-HA were the same in all three strains (Fig. 5A and B), indicating that a defect in Pmt1p and Pmt2p does not affect the rate of degradation of non-*O*-mannosylated ERAD substrates. Therefore, stabilization of Gas1*p might not result from general ER stress due to the *PMT* deletions but instead, might be attributable to a defect in *O*-mannosylation.

*Gas1*p is Targeted to the Vacuole via Endosomes in* pmt1Δ pmt2Δ *Double-Mutant Cells*—Previous studies reported that some misfolded proteins that are degraded by vacuolar proteases are targeted to vacuoles *via* two pathways, the Golgi-to-vacuole pathway (*9*, *13*, *49*) and the autophagic pathway (*12*, *13*, *50*, *51*). Additionally, ER-to-Golgi trafficking of Gas1*p is required for proteasome-dependent degradation (*35*). Thus, we hypothesized that Gas1*p is transported to the vacuole *via* the Golgi apparatus. To address this possibility, we analysed the kinetics of degradation of HA-Gas1*p in *vps38* deletion mutant cells. Vps38p is a component of the Vps30 Complex II (Vps15p–Vps34p–Vps38p–Vps30p complex), which recruits and stimulates the phosphatidylinositol 3-kinase Vps34p. Vps34p kinase activity in endosomal membranes is required for proper sorting of some vacuole-targeted proteins from the Golgi to vacuoles (*52*). As shown in Fig. 6, we found that degradation of HA-Gas1*p was significantly reduced in *vps38*Δ *pmt1*Δ *pmt2*Δ cells as compared to its degradation in wild-type or *vps38*Δ single-mutant cells. Furthermore, the degree of HA-Gas1*p stabilization in *vps38*Δ *pmt1*Δ *pmt2*Δ cells was similar to that of stabilization observed in *pep4*Δ *pmt1*Δ *pmt2*Δ cells (Fig. 3B). This suggests that HA-Gas1*p enters the Golgi-to-vacuole pathway *via* endosomes and that targeting of HA-Gas1*p to the vacuole depends on the *VPS30* complex II in *pmt1*Δ *pmt2*Δ cells (see DISCUSSION section).

*Gas1*p Forms a Weakly Aggregated Oligomer in* pep4Δ pmt1Δ pmt2Δ *Triple Mutant Cells*—The above observations prompted us to examine why HA-Gas1*p is degraded by vacuolar protease when expressed in *pmt1*Δ *pmt2*Δ cells but not when expressed in wild-type or *pmt4*Δ *pmt6*Δ cells (Fig. 3A and B). We reasoned that HA-Gas1*p expressed in *pmt1*Δ *pmt2*Δ cells aggregates in the ER and that aggregated HA-Gas1*p can be transported to the vacuole to be degraded. This hypothesis is partially supported by the finding that *O*-mannosylation enhances solubility and suppresses aggregation of several *O*-mannosylated misfolded

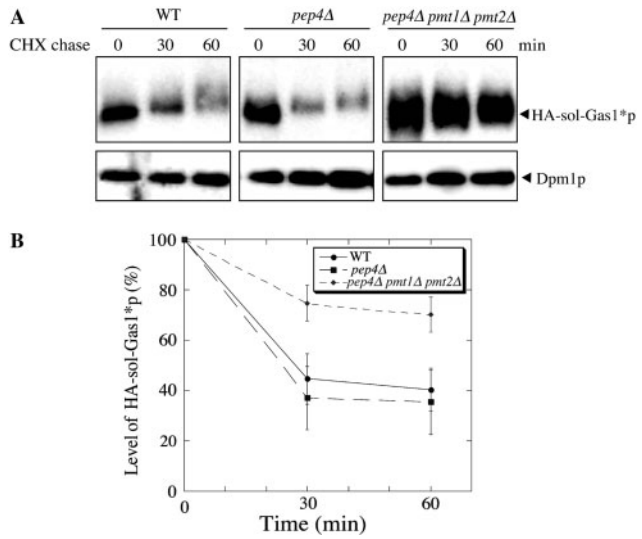

Fig. 4. **HA-sol-Gas1*p is also degraded in the vacuole in *pmt1Δ pmt2Δ* double-mutant cells.** (A) CHX-chase experiment in wild-type (YME1398), *pep4*Δ (YME1399) and *pep4*Δ *pmt1*Δ *pmt2*Δ (YME1400) cells expressing HA-sol-Gas1*p. Exponentially-grown cells were incubated with 200 μg/ml of CHX, and 1.0 OD_{600} unit of cells were recovered at the indicated time points. Then 5 μl of each sample was separated by SDS–PAGE and analysed by immunoblotting with anti-HA antibody. The immunoblot was subsequently probed with anti-Dpm1p as a control for protein loading. (B) The relative amounts of HA-sol-Gas1*p were quantified with an image analyser and plotted as mean values ± SD from three independent experiments, with the quantity at the 0 time point set at 100%.

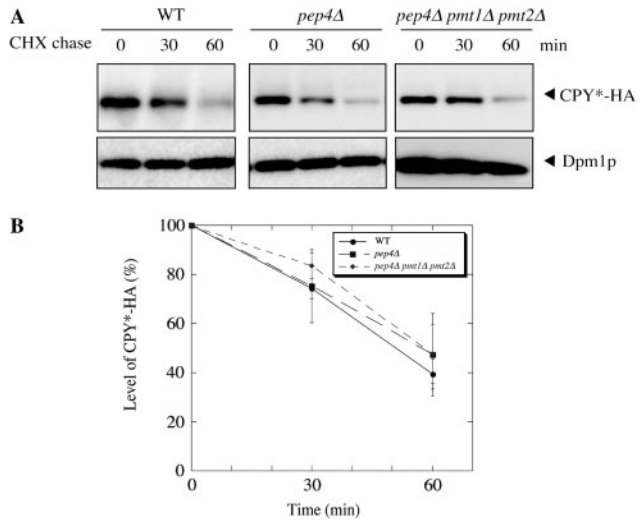

Fig. 5. **Deletion of *PEP4* has no effect on degradation of CPY* in *pmt1Δ pmt2Δ* cells.** (A) CHX-chase experiment of CPY*-HA expressed in wild-type (YME1421), *pep4*Δ (YME1422) and *pep4*Δ *pmt1*Δ *pmt2*Δ (YME1423) cells. Five OD_{600} units of cells were recovered at the indicated time points. Then 5 μl of each sample was separated by SDS–PAGE and analysed by immunoblotting as described in Fig. 4A. (B) The relative amounts of CPY*-HA were quantified as described in Fig. 4B.

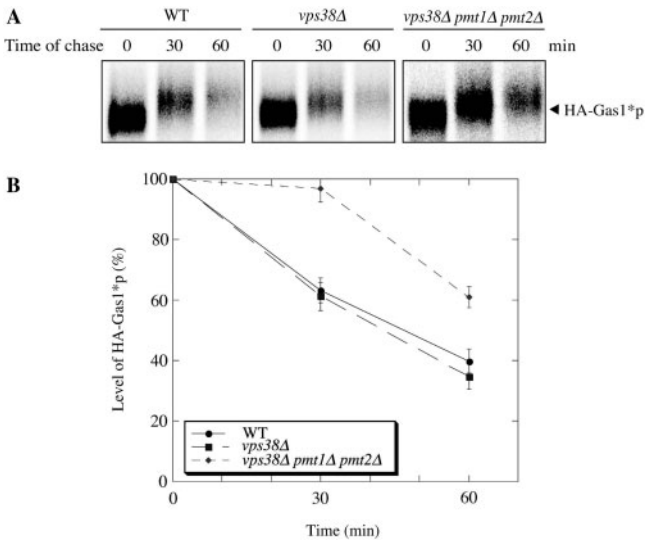

Fig. 6. **Degradation of HA-Gas1*p is reduced in *vps38Δ pmt1Δ pmt2Δ* cells.** (A) HA-Gas1*p expressed in wild-type (YME1305), *vps38*Δ (YME1444) and *vps38*Δ *pmt1*Δ *pmt2*Δ (YME1440) cells were pulse-labelled with [^{35}S]-cysteine/methionine as described in Fig. 3. (B) The relative amounts of HA-Gas1*p were quantified as described in Fig. 3. Error bars indicate means values ± SD from three independent experiments.

proteins, including mutant pαF and Δpro (*32*). Moreover, it was recently reported that the aggregation-competent Z variant of human α-1 proteinase inhibitor (A1PiZ) is targeted to the vacuole when it is expressed in yeast cells (*13*). To address whether HA-Gas1*p forms an aggregate in *O*-mannosylation defective cells, we monitored the level of aggregated HA-sol-Gas1*p derived from wild-type, *pep4*Δ and *pep4*Δ *pmt1*Δ *pmt2*Δ cells separated by sucrose density centrifugation. GPI-anchored Gas1*p could not be fractionated on the sucrose density gradient, presumably because Gas1*p tends to be insoluble due to the lipid moiety of the GPI-anchor. Therefore, we used HA-sol-Gas1*p, which, like HA-Gas1*p, is *O*-mannosylated by Pmt1p and Pmt2p (Fig. 2C); is excessively *O*-mannosylated compared with sol-Gas1p (Fig. 1C); and is stabilized when expressed in *pep4*Δ *pmt1*Δ *pmt2*Δ triple-mutant cells (Fig. 4). As shown in Fig. 7, sol-Gas1*p was not observed in the bottom fraction, different from other aggregated-prone misfolded proteins (*13*, *32*). By contrast, we found that the distribution of HA-sol-Gas1*p expressed in *pep4*Δ *pmt1*Δ *pmt2*Δ cells was shifted slightly, appearing in a higher molecular weight fraction than it does in a wild-type background (Fig. 7A). Especially, the relative amount of HA-sol-Gas1*p in *pep4*Δ *pmt1*Δ *pmt2*Δ triple-mutant cells in fraction 4–6 is increased as compared with those of wild-type and *pep4*Δ mutant cells (Fig. 7B; the region of horizontal bracket). This result suggests that HA-sol-Gas1*p does not aggregate severely, but does form a weakly aggregated oligomer (small aggregate) in *pmt1*Δ *pmt2*Δ double-mutant cells.

The Rate of Degradation of KHNt is Significantly Reduced in pmt1Δ pmt2Δ *Cells, Irrespective of Pep4p Function*—We examined whether other misfolded model

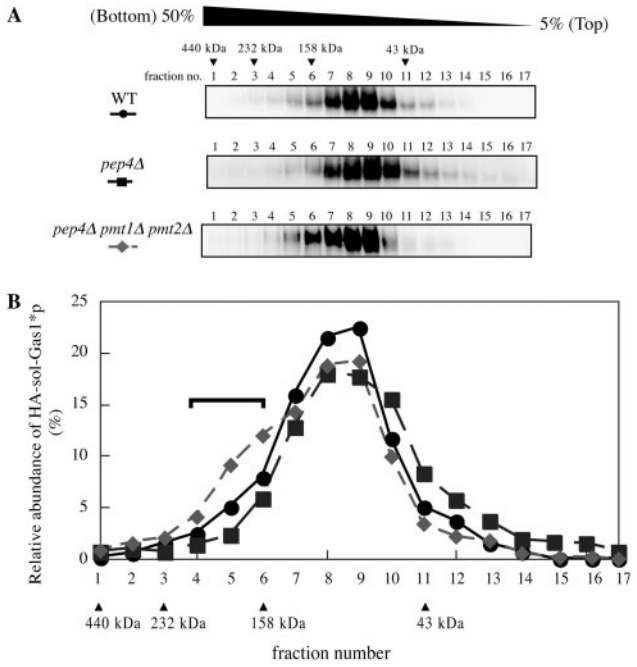

Fig. 7. **HA-sol-Gas1*p expressed in *pep4*Δ *pmt1*Δ *pmt2*Δ cells was more aggregated than that in wild-type and *pep4*Δ cells.** (A) Whole-cell lysates were prepared from HA-sol-Gas1*p expressing wild-type (YME1398), *pep4*Δ (YME1399) and *pep4*Δ *pmt1*Δ *pmt2*Δ (YME1400) cells. Cell lysates were subjected to 5–50% linear sucrose density gradient centrifugation. Fractions (200 µl each) were collected and analysed by SDS–PAGE, followed by immunoblotting using an anti-HA antibody (1:8,000) and HRP-conjugated anti-mouse IgG antibody (1:8,000) (see MATERIALS AND METHODS section). (B) Relative amounts of HA-sol-Gas1*p in each fraction were quantified. Vertical arrowheads indicate the position of ferritin (440 kDa), catalase (232 kDa), aldolase (158 kDa) and ovalbumin (43 kDa), respectively.

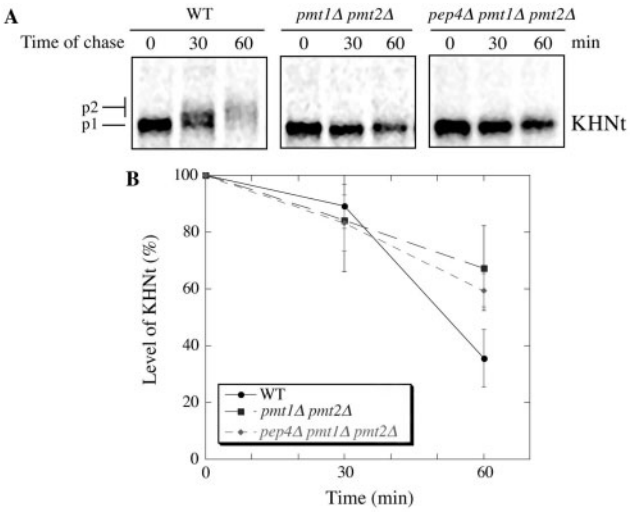

Fig. 8. **The rate of degradation of KHNt is reduced in *pmt1*Δ *pmt2*Δ cells.** (A) KHNt expressed in wild-type (YME1445), *pmt1*Δ *pmt2*Δ (YME1446) and *pep4*Δ *pmt1*Δ *pmt2*Δ (YME1447) cells were pulse-labelled with [^{35}S]-cysteine/methionine as described in Fig. 3. The p1 and p2 refer to ER form and Golgi form of KHNt, respectively. (B) The relative amounts of KHNt were quantified as described in Fig. 3. Error bars indicate means values ± SD from three independent experiments.

proteins that are *O*-mannosylated in their misfolded status behave as Gas1*p in cells where *PMT1* and *PMT2* were deleted. We chose a model misfolded protein KHNt (HA-tagged yeast Kar2p signal sequence fusion to simian virus 5 haemagglutinin neuraminidase), which is known to be *O*-mannosylated by Pmt1p and Pmt2p (*33*). Pulse-chase experiment revealed that the deletion of both *PMT1* and *PMT2* resulted in a decreased rate of KHNt degradation, regardless of *pep4*Δ mutation (Fig. 8A and B). Thus, we further examined whether KHNt is defective in its transport from the ER-to-Golgi due to the formation of severe aggregates of KHNt in the ER in *pmt1*Δ *pmt2*Δ mutant cells, using the sucrose density gradient and detergent fractionation assays. As shown in Fig. 9A and B, a large amount of KHNt was observed in the bottom fraction of sucrose density gradient in *pmt1*Δ *pmt2*Δ mutant cells, indicating that KHNt was aggregated. In sucrose density gradient of wild-type cell lysates, we could not detect Golgi form of KHNt (see p2 form of Fig. 8A). Since previous report suggests that the Golgi form of KHNt is preferentially degraded in wild-type cells (*33*), it is reasonable that Golgi form of KHNt could not be detected presumably because of its small amount or degradation during fractionation step. In detergent-partition assay using Triton X-100, both KHNt expressed in *pmt1*Δ *pmt2*Δ and *pep4*Δ *pmt1*Δ *pmt2*Δ mutant cells showed a detergent-insoluble aggregated form (Fig. 9C), whereas HA-sol-Gas1*p did not form a detergent-insoluble aggregate under the same condition (data not shown). These results indicate that the rate of degradation of KHNt was significantly reduced due to their severe aggregation, suggesting that the behaviour of KHNt is different from that of Gas1*p in *pmt1*Δ *pmt2*Δ double-mutant cells.

DISCUSSION

In this report, we dissected the role of *O*-mannosylation in the intracellular quality-control machinery using the misfolded protein Gas1*p. We showed that Gas1*p is excessively *O*-mannosylated by Pmt1p and Pmt2p as compared to correctly folded Gas1p. We also found that HA-Gas1*p is transported to the vacuole *via* the Golgi and endosomes, and degraded by vacuolar proteases only when protein *O*-mannosylation that is executed by Pmt1p and Pmt2p is abolished. Our data suggest that Pmt1p and Pmt2p are important for proteasome-dependent degradation of Gas1*p. In wild-type cells, Gas1*p is primarily degraded by ERAD pathway. The balance of the operated pathways could be changed such that Gas1*p is degraded mainly by the vacuolar-dependent pathway when *PMT1* and *PMT2* are deleted, although it is still unclear if the contribution by ERAD pathway is completely abolished in these circumstances. Thus, we hypothesize that *O*-mannosylation by Pmt1p and Pmt2p is an important step in the targeting of

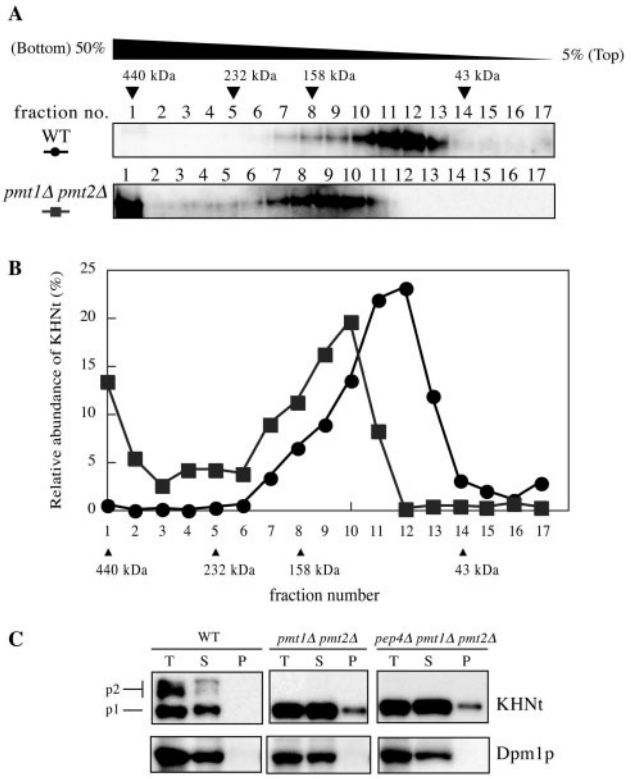

Fig. 9. **KHNt forms detergent-insoluble aggregates in *pmt1*Δ *pmt2*Δ cells.** (A) Whole-cell lysates were prepared from KHNt expressing wild-type (YME1445) and *pmt1*Δ *pmt2*Δ (YME1446) cells. Cell lysates (300 μg of protein) were subjected to 5–50% linear sucrose density gradient centrifugation. Fractions (150 μl each) were collected and analysed by SDS–PAGE, followed by Immunoblotting using an anti-HA antibody (1:4,000) and HRP-conjugated anti-mouse IgG antibody (1:4,000) (see MATERIALS AND METHODS section). Relative amounts of KHNt in each fraction were quantified. Vertical arrowheads indicate the position of ferritin (440 kDa), catalase (232 kDa), aldolase (158 kDa) and ovalbumin (43 kDa), respectively. (B) Relative amounts of KHNt in each fraction were quantified. Vertical arrowheads indicate the position of ferritin (440 kDa), catalase (232 kDa), aldolase (158 kDa) and ovalbumin (43 kDa), respectively. (C) Membrane fractions of YME1445, YME1446 and YMT1447 strains were solubilized in 1% Triton X-100 and separated into pellet and supernatant fractions by centrifugation (see MATERIALS AND METHODS section). Total (T), detergent-soluble (S) and detergent-insoluble pellet (P) fractions were resolved by SDS–PAGE, followed by immunoblot using an anti-HA antibody (1:10,000) and HRP-conjugated anti-mouse IgG antibody (1:10,000). The extent of membrane solubilization was determined by immunoblot of Dpm1p using anti-Dpm1p antibody (1:5,000) followed by HRP-conjugated anti-mouse IgG antibody (1:10,000). The p1 and p2 refer to ER form and Golgi form of KHNt, respectively.

Gas1*p for degradation *via* the proteasome-dependent ERAD pathway.

ERAD substrates including mutant pαF and Δpro seem to be less soluble than correctly folded proteins (*32*). Mutant pαF, Δpro and KHNt are modified with highly hydrophilic *O*-mannosyl sugar chains to make them more soluble. It is noteworthy that Gas1*p is not likely a solubility-reduced ERAD substrate because Gas1*p is highly glycosylated in the ER (the molecular weight of the primary translated form of Gas1*p is 65 kDa and that of the glycosylated form is ~100 kDa), in contrast to other *O*-mannosylated misfolded proteins. In the experiment using *pep4*Δ *pmt1*Δ or *pep4*Δ *pmt2*Δ double-mutant cells, the degradation rate of Gas1*p is not reduced to the same extent as that of Gas1*p expressed in *pep4*Δ *pmt1*Δ *pmt2*Δ cells (our unpublished data), presumably due to the compensation of defect in Pmt1p and/or Pmt2p functions by Pmt3p or Pmt5p (*25*). After co-translational *O*-mannosylation by Pmt4p and Pmt6p, Gas1*p-specific *O*-mannosylation, which is mediated by Pmt1p and Pmt2p, may occur post-translationally near the amino acid-substituted region (G291R), in which the polypeptide is unfolded and internal hydrophobic amino acids may be exposed on the surface of the protein. It is likely that *O*-mannoses are transferred to serine or threonine residues adjacent to the unfolded region of Gas1*p such that they alleviate aggregation due to hydrophobic interactions, helping to reduce or eliminate accumulation of misfolded proteins in the ER. Another possibility is that *O*-mannosylation mediated by Pmt1p and Pmt2p may act as a retrieval signal from the Golgi to the ER in ERAD-L pathway (*33*, *35*, *53*) or act as a tag for the recognition by ERAD machinery.

Two pathways have been reported for the transport of aggregated, misfolded proteins to the vacuole in yeast. One is the Golgi-to-vacuole sorting pathway (*9*, *13*, *49*). The other is the autophagic pathway (*12*, *13*, *50*, *51*). Several reports suggest that the route of vacuolar targeting in post-ER degradation is substrate-specific. For Gas1*p transport to the vacuole, the Vps30p complex II is essential for Golgi-to-vacuole sorting *via* endosomes. We could not clearly determine if the autophagic pathway is also used to target Gas1*p to the vacuole using the mutant cell of *ATG14*, which is an essential subunit of *VPS30* complex I (Vps15p–Vps34p–Atg14p–Vps30p complex) for autophagy, due to the severe growth defect of *atg14*Δ *pmt1*Δ *pmt2*Δ triple-mutant cells. However, the degradation kinetics of Gas1*p in *vps38*Δ *pmt1*Δ *pmt2*Δ cells resembled that in *pep4*Δ *pmt1*Δ *pmt2*Δ cells (Fig. 3B and 6B) and Gas1*p was not so severely aggregated as compared with misfolded proteins which are transported to vacuole *via* autophagic pathway; namely, A1PiZ, mutant fibrinogen and mutant dysferlin, (*12–14*). Therefore, it is conceivable that a large proportion of Gas1*p is targeted to the vacuole *via* the Golgi apparatus in *pmt1*Δ *pmt2*Δ cells. We addressed whether Vps10p, a Golgi-to-vacuole sorting receptor of some vacuolar proteins, is involved in the sorting of Gas1*p, but found that the rate of degradation of Gas1*p was not reduced in *vps10*Δ or *vps10*Δ *pmt1*Δ *pmt2*Δ mutant cells (our unpublished data). Taken together, the data suggest that Gas1*p and sol-Gas1*p may be sorted by a Golgi-to-vacuole sorting receptor other than Vps10p.

We fractionated sol-Gas1*p by sucrose density gradient centrifugation and observed a weakly aggregated sol-Gas1*p oligomer (Fig. 7; it should be noted that GPI-anchored Gas1*p could not be fractionated). We could not clearly distinguish differences in aggregation of GPI-anchored Gas1*p in wild-type, *pep4*Δ or *pep4*Δ *pmt1*Δ *pmt2*Δ cells. However, both sol-Gas1*p and Gas1*p contain more *O*-mannosylated serine/threonine

residues than each of correctly folded forms (sol-Gas1p and Gas1p, respectively; Fig. 1) and as for Gas1*p, degradation of sol-Gas1*p was delayed in *pep4*Δ *pmt1*Δ *pmt2*Δ cells (Fig. 4). Therefore, it is conceivable that Gas1*p, which contains a GPI anchor, also behaves like sol-Gas1*p in *pep4*Δ *pmt1*Δ *pmt2*Δ triple-mutant cells. The degree to which sol-Gas1*p aggregated is significantly less than what was observed for another *O*-mannosylated misfolded protein KHNt in Pmt1p and Pmt2p defective cells (Fig. 9). Because sol-Gas1*p is highly glycosylated and more soluble than other *O*-mannosylated misfolded proteins in their misfolded state, it seems reasonable that, different from other misfolded proteins, sol-Gas1*p was not present in large amounts in the fraction adjacent to the bottom fraction. Therefore, Gas1*p serves as an unique model *O*-mannosylated misfolded protein, distinct from previously reported model proteins which take *O*-mannosylation under their misfolded status. From these differences between Gas1*p and KHNt, we propose a hypothesis that misfolded proteins that are *O*-mannosylated in their misfolded status can be classified into at least two types in view of the degree of aggregation. Proteins in the first class of misfolded proteins, including KHNt, accumulate as a large aggregate in the ER when both *PMT1* and *PMT2* are defective. Proteins in the second class of misfolded proteins, including Gas1*p, form a small aggregated oligomer but can exit the ER. However, it remains unclear whether the degradation of previously reported two misfolded proteins Δpro and mutant pαF, which are *O*-mannosylated under their misfolded status, are subjected to vacuolar proteases-dependent degradation when the function of Pmt1p and Pmt2p are abolished, because mutant pαF has been used as a model for misfolded proteins only for the *in vitro* ERAD assay system (*31*, *54*, *55*), and because Δpro is mannosylated only when the component of ERAD machinery is deleted (for example, in *der1*Δ or *cue1*Δ mutant) (*32*).

Although we found that the excessive *O*-mannosylation of Gas1*p by Pmt1p and Pmt2p is important for proteasome-dependent degradation, several questions remained unsolved. For example, does Pmt1p–Pmt2p complex or additional other factors recognize unfolded region of misfolded proteins? Which Ser/Thr sites in Gas1*p are specifically *O*-mannosylated by Pmt1p and Pmt2p? Are there any lectin-like receptors, which can recognize misfolded protein-specific *O*-mannosylation? Further studies to address these questions are necessary to understand better the physiological function of *O*-mannosylation of misfolded proteins.

We are grateful to Dr Davis Ng (National University of Singapore, Singapore) for providing the pSM70 plasmid (KHNt expression vector); to Dr Shu-ichi Nishikawa (Nagoya University, Nagoya, Japan) for the pUC18-Mfα plasmid; to Dr Kazutoshi Mori (Kyoto University, Kyoto, Japan) for the UPR reporter assay plasmid (pSCZ-Y); and to Dr Katsura Hata (Eisai Co.) for the anti-Gas1p peptide polyclonal antibody. We also thank Dr Takuji Oka, Mr Toshihiko Kitajima, Ms Michiyo Okamoto, Dr Yasunori Chiba and Dr Yoh-ichi Shimma for guidance with experiments and helpful discussions.

REFERENCES

1. Bucciantini, M., Giannoni, E., Chiti, F., Baroni, F., Formigli, L., Zurdo, J., Taddei, N., Ramponi, G., Dobson, C.M., and Stefani, M. (2002) Inherent toxicity of aggregates implies a common mechanism for protein misfolding diseases. *Nature* **416**, 507–511
2. Helenius, A. and Aebi, M. (2004) Roles of *N*-linked glycans in the endoplasmic reticulum. *Annu. Rev. Biochem.* **73**, 1019–1049
3. Helenius, A. and Aebi, M. (2001) Intracellular functions of *N*-linked glycans. *Science* **291**, 2364–2369
4. Ellgaard, L., Molinari, M., and Helenius, A. (1999) Setting the standards: quality control in the secretory pathway. *Science* **286**, 1882–1888
5. Kostova, Z. and Wolf, D.H. (2005) Importance of carbohydrate positioning in the recognition of mutated CPY for ER-associated degradation. *J. Cell. Sci.* **118**, 1485–1492
6. Xu, X., Azakami, H., and Kato, A. (2004) P-domain and lectin site are involved in the chaperone function of *Saccharomyces cerevisiae* calnexin homologue. *FEBS Lett.* **570**, 155–160
7. Kopito, R.R. (1997) ER quality control: the cytoplasmic connection. *Cell* **88**, 427–430
8. Kostova, Z. and Wolf, D.H. (2003) For whom the bell tolls: protein quality control of the endoplasmic reticulum and the ubiquitin-proteasome connection. *EMBO J.* **22**, 2309–2317
9. Coughlan, C.M., Walker, J.L., Cochran, J.C., Wittrup, K.D., and Brodsky, J.L. (2004) Degradation of mutated bovine pancreatic trypsin inhibitor in the yeast vacuole suggests post-endoplasmic reticulum protein quality control. *J. Biol. Chem.* **279**, 15289–15297
10. Jorgensen, M.U., Emr, S.D., and Winther, J.R. (1999) Ligand recognition and domain structure of Vps10p, a vacuolar protein sorting receptor in *Saccharomyces cerevisiae*. *Eur. J. Biochem.* **260**, 461–469
11. Arvan, P., Zhao, X., Ramos-Castaneda, J., and Chang, A. (2002) Secretory pathway quality control operating in Golgi, plasmalemmal, and endosomal systems. *Traffic* **3**, 771–780
12. Fujita, E., Kouroku, Y., Isoai, A., Kumagai, H., Misutani, A., Matsuda, C., Hayashi, Y.K., and Momoi, T. (2007) Two endoplasmic reticulum-associated degradation (ERAD) systems for the novel variant of the mutant dysferlin: ubiquitin/proteasome ERAD (I) and autophagy/lysosome ERAD (II). *Hum. Mol. Genet.* **16**, 618–629
13. Kruse, K.B., Brodsky, J.L., and McCracken, A.A. (2006) Characterization of an ERAD gene as *VPS30/ATG6* reveals two alternative and functionally distinct protein quality control pathways: one for soluble Z variant of human alpha-1 proteinase inhibitor (A1PiZ) and another for aggregates of A1PiZ. *Mol. Biol. Cell* **17**, 203–212
14. Kruse, K.B., Dear, A., Kaltenbrun, E.R., Crum, B.E., George, P.M., Brennan, S.O., and McCracken, A.A. (2006) Mutant fibrinogen cleared from the endoplasmic reticulum via endoplasmic reticulum-associated protein degradation and autophagy: an explanation for liver disease. *Am. J. Pathol.* **168**, 1299–1308;quiz 1404–1295
15. Conibear, E. and Stevens, T.H. (1998) Multiple sorting pathways between the late Golgi and the vacuole in yeast. *Biochim. Biophys. Acta* **1404**, 211–230
16. Klionsky, D.J. and Emr, S.D. (2000) Autophagy as a regulated pathway of cellular degradation. *Science* **290**, 1717–1721
17. Willer, T., Valero, M.C., Tanner, W., Cruces, J., and Strahl, S. (2003) *O*-mannosyl glycans: from yeast to novel associations with human disease. *Curr. Opin. Struct. Biol.* **13**, 621–630

18. Martin-Blanco, E. and Garcia-Bellido, A. (1996) Mutations in the rotated abdomen locus affect muscle development and reveal an intrinsic asymmetry in *Drosophila*. *Proc. Natl Acad. Sci. USA* **93**, 6048–6052
19. Strahl-Bolsinger, S., Immervoll, T., Deutzmann, R., and Tanner, W. (1993) *PMT1*, the gene for a key enzyme of protein *O*-glycosylation in *Saccharomyces cerevisiae*. *Proc. Natl Acad. Sci. USA* **90**, 8164–8168
20. Strahl-Bolsinger, S., Gentzsch, M., and Tanner, W. (1999) Protein *O*-mannosylation. *Biochim. Biophys. Acta* **1426**, 297–307
21. VanderVen, B.C., Harder, J.D., Crick, D.C., and Belisle, J.T. (2005) Export-mediated assembly of mycobacterial glycoproteins parallels eukaryotic pathways. *Science* **309**, 941–943
22. Oka, T., Hamaguchi, T., Sameshima, Y., Goto, M., and Furukawa, K. (2004) Molecular characterization of protein *O*-mannosyltransferase and its involvement in cell-wall synthesis in *Aspergillus nidulans*. *Microbiology* **150**, 1973–1982
23. Orlean, P. (1990) Dolichol phosphate mannose synthase is required in vivo for glycosyl phosphatidylinositol membrane anchoring, *O* mannosylation, and *N* glycosylation of protein in *Saccharomyces cerevisiae*. *Mol. Cell Biol.* **10**, 5796–5805
24. Girrbach, V. and Strahl, S. (2003) Members of the evolutionarily conserved *PMT* family of protein *O*-mannosyltransferases form distinct protein complexes among themselves. *J. Biol. Chem.* **278**, 12554–12562
25. Gentzsch, M. and Tanner, W. (1997) Protein-*O*-glycosylation in yeast: protein-specific mannosyltransferases. *Glycobiology* **7**, 481–486
26. Weber, Y., Prill, S.K., and Ernst, J.F. (2004) Pmt-mediated *O* mannosylation stabilizes an essential component of the secretory apparatus, Sec20p, in *Candida albicans*. *Eukaryot. Cell* **3**, 1164–1168
27. Lommel, M., Bagnat, M., and Strahl, S. (2004) Aberrant processing of the *WSC* family and Mid2p cell surface sensors results in cell death of *Saccharomyces cerevisiae O*-mannosylation mutants. *Mol. Cell. Biol.* **24**, 46–57
28. Proszynski, T.J., Simons, K., and Bagnat, M. (2004) *O*-glycosylation as a sorting determinant for cell surface delivery in yeast. *Mol. Biol. Cell* **15**, 1533–1543
29. Gentzsch, M. and Tanner, W. (1996) The *PMT* gene family: protein *O*-glycosylation in *Saccharomyces cerevisiae* is vital. *EMBO J.* **15**, 5752–5759
30. Sanders, S.L., Gentzsch, M., Tanner, W., and Herskowitz, I. (1999) *O*-Glycosylation of Axl2/Bud10p by Pmt4p is required for its stability, localization, and function in daughter cells. *J. Cell. Biol.* **145**, 1177–1188
31. Harty, C., Strahl, S., and Romisch, K. (2001) *O*-mannosylation protects mutant alpha-factor precursor from endoplasmic reticulum-associated degradation. *Mol. Biol. Cell* **12**, 1093–1101
32. Nakatsukasa, K., Okada, S., Umebayashi, K., Fukuda, R., Nishikawa, S., and Endo, T. (2004) Roles of *O*-mannosylation of aberrant proteins in reduction of the load for endoplasmic reticulum chaperones in yeast. *J. Biol. Chem.* **279**, 49762–49772
33. Vashist, S., Kim, W., Belden, W.J., Spear, E.D., Barlowe, C., and Ng, D.T. (2001) Distinct retrieval and retention mechanisms are required for the quality control of endoplasmic reticulum protein folding. *J. Cell Biol.* **155**, 355–368
34. Mouyna, I., Fontaine, T., Vai, M., Monod, M., Fonzi, W.A., Diaquin, M., Popolo, L., Hartland, R.P., and Latge, J.P. (2000) Glycosylphosphatidylinositol-anchored glucanosyltransferases play an active role in the biosynthesis of the fungal cell wall. *J. Biol. Chem.* **275**, 14882–14889
35. Fujita, M., Yoko-o, T., and Jigami, Y. (2006) Inositol deacylation by Bst1p is required for the quality control of glycosylphosphatidylinositol-anchored proteins. *Mol. Biol. Cell* **17**, 834–850
36. Longtine, M.S., McKenzie, A III, Demarini, D.J., Shah, N.G., Wach, A., Brachat, A., Philippsen, P., and Pringle, J.R. (1998) Additional modules for versatile and economical PCR-based gene deletion and modification in *Saccharomyces cerevisiae*. *Yeast* **14**, 953–961
37. Sherman, F. (1991) Getting started with yeast. *Methods Enzymol.* **194**, 3–21
38. Sikorski, R.S. and Hieter, P. (1989) A system of shuttle vectors and yeast host strains designed for efficient manipulation of DNA in *Saccharomyces cerevisiae*. *Genetics* **122**, 19–27
39. Okamoto, M., Yoko-o, T., Umemura, M., Nakayama, K., and Jigami, Y. (2006) Glycosylphosphatidylinositol-anchored proteins are required for the transport of detergent-resistant microdomain-associated membrane proteins Tat2p and Fur4p. *J. Biol. Chem.* **281**, 4013–4023
40. Spear, E.D. and Ng, D.T. (2005) Single, context-specific glycans can target misfolded glycoproteins for ER-associated degradation. *J. Cell. Biol.* **169**, 73–82
41. Vai, M., Gatti, E., Lacana, E., Popolo, L., and Alberghina, L. (1991) Isolation and deduced amino acid sequence of the gene encoding gp115, a yeast glycophospholipid-anchored protein containing a serine-rich region. *J. Biol. Chem.* **266**, 12242–12248
42. Popolo, L. and Vai, M. (1999) The Gas1 glycoprotein, a putative wall polymer cross-linker. *Biochim. Biophys. Acta* **1426**, 385–400
43. Taxis, C., Vogel, F., and Wolf, D.H. (2002) ER-golgi traffic is a prerequisite for efficient ER degradation. *Mol. Biol. Cell* **13**, 1806–1818
44. Lussier, M., Sdicu, A.M., Bussereau, F., Jacquet, M., and Bussey, H. (1997) The Ktr1p, Ktr3p, and Kre2p/Mnt1p mannosyltransferases participate in the elaboration of yeast *O*- and *N*-linked carbohydrate chains. *J. Biol. Chem.* **272**, 15527–15531
45. Hutzler, J., Schmid, M., Bernard, T., Henrissat, B., and Strahl, S. (2007) Membrane association is a determinant for substrate recognition by *PMT4* protein *O*-mannosyltransferases. *Proc. Natl Acad. Sci. USA* **104**, 7827–7832
46. Kincaid, M.M. and Cooper, A.A. (2007) Misfolded proteins traffic from the endoplasmic reticulum (ER) due to ER export signals. *Mol. Biol. Cell* **18**, 455–463
47. Finger, A., Knop, M., and Wolf, D.H. (1993) Analysis of two mutated vacuolar proteins reveals a degradation pathway in the endoplasmic reticulum or a related compartment of yeast. *Eur. J. Biochem.* **218**, 565–574
48. Knop, M., Hauser, N., and Wolf, D.H. (1996) *N*-Glycosylation affects endoplasmic reticulum degradation of a mutated derivative of carboxypeptidase yscY in yeast. *Yeast* **12**, 1229–1238
49. Holkeri, H. and Makarow, M. (1998) Different degradation pathways for heterologous glycoproteins in yeast. *FEBS Lett.* **429**, 162–166
50. Mazon, M.J., Eraso, P., and Portillo, F. (2007) Efficient degradation of misfolded mutant Pma1 by endoplasmic reticulum-associated degradation requires Atg19 and the Cvt/autophagy pathway. *Mol. Microbiol.* **63**, 1069–1077
51. Kamimoto, T., Shoji, S., Hidvegi, T., Mizushima, N., Umebayashi, K., Perlmutter, D.H., and Yoshimori, T. (2006) Intracellular inclusions containing mutant alpha1-antitrypsin Z are propagated in the absence of autophagic activity. *J. Biol. Chem.* **281**, 4467–4476
52. Odorizzi, G., Babst, M., and Emr, S.D. (2000) Phosphoinositide signaling and the regulation of membrane trafficking in yeast. *Trends Biochem. Sci.* **25**, 229–235

53. Nishikawa, S., Brodsky, J.L., and Nakatsukasa, K. (2005) Roles of molecular chaperones in endoplasmic reticulum (ER) quality control and ER-associated degradation (ERAD). *J. Biochem.* **137**, 551–555
54. McCracken, A.A. and Brodsky, J.L. (1996) Assembly of ER-associated protein degradation in vitro: dependence on cytosol, calnexin, and ATP. *J. Cell Biol.* **132**, 291–298
55. Pilon, M., Schekman, R., and Romisch, K. (1997) Sec61p mediates export of a misfolded secretory protein from the endoplasmic reticulum to the cytosol for degradation. *EMBO J.* **16**, 4540–4548
56. Sutton, A., Immanuel, D., and Arndt, K.T. (1991) The *SIT4* protein phosphatase functions in late G1 for progression into S phase. *Mol. Cell Biol.* **11**, 2133–2148